Original software publication

OpenArch: An open-source package for determining the minimum-thickness of arches under seismic loads

Thomas McLean [a], Christian Málaga-Chuquitaype [a,*], Nicos Kalapodis [b], Georgios Kampas [b]

[a] *Department of Civil and Environmental Engineering, Imperial College London, UK*
[b] *School of Engineering, University of Greenwich, UK*

ARTICLE INFO

ABSTRACT

Arches are elegant and efficient structural forms that can be used in a wide variety of applications, from bridges to extraterrestrial shielding structures. Oftentimes their design hinges around the identification of the minimum-thickness required to ensure their stability when subjected to gravity and lateral (inertial) loading. This work presents a MATLAB-based code called OpenArch developed within a procedural programming framework for the preliminary design and assessment of optimal arch forms of minimum thickness when subjected to combined self-weight and seismically induced loads. The code, which is based on limit thrust-line analysis can handle any classical or non-classical no-tension arch form and the results compare excellently with the few available analytical solutions.

© 2021 Published by Elsevier B.V. This is an open access article under the CC BY license (http://creativecommons.org/licenses/by/4.0/).

Code metadata

Current code version	Version 1.0
Permanent link to code/repository used for this code version	https://github.com/ElsevierSoftwareX/SOFTX-D-21-00053
Code Ocean compute capsule	none
Legal Code License	GNU GPLv3
Code versioning system used	none
Software code languages, tools, and services used	MATLAB
Compilation requirements, operating environments & dependencies	Windows, Mac OS, the MATLAB package requires MATLAB 2017b and above
If available Link to developer documentation/manual	https://github.com/CMalagaC/OpenArch/tree/main/Documentation
Support email for questions	thomas.o.mclean@outlook.com

1. Motivation and significance

Arches are widely used as structural elements in the construction of coverings for open spaces where they can be subjected to lateral and vertical actions from seismic events. These loads are usually represented by mass-proportional static forces during preliminary assessments, an approach that is also adopted herein Although arches have been the subject of intensive analysis since the XVII Century, there is much less research on their optimal shape when subjected to horizontal seismic loads; and, to the

authors' knowledge, only a handful of studies have dealt with this. By contrast, a large amount of research has been carried out on the analysis of masonry arches subjected to vertical loads. In this context, the optimal shape of a masonry arch is often associated with the catenary [1,2]. This is despite proofs offered by Milankowitch [3] and Makris and Alexakis [4] who demonstrated that, apart from 1D arches, admissible thrust-lines cannot be of catenary shape, hence an arch of finite thickness that resembles a catenary cannot be automatically assumed as optimal. Moreover, it has been proven that there is no minimum thickness associated with a catenary arch under its own weight [5].

Past studies have mostly examined the stability of arches of classical form under static loads through analytical procedures

---

* Corresponding author.
E-mail address: c.malaga@imperial.ac.uk (Christian Málaga-Chuquitaype).

[1,3,4,6–8] or numerical techniques [9–11]. However, these analysis have usually been constrained to circular arches of uniform thickness. In his seminal work, Oppenheim [12] formulated the equations of motion for circular arches under base motion assuming eight radial joints. Although the collapse mechanism of a masonry arch is rightly associated with a minimum horizontal acceleration for a given thickness, the definition of a pre-defined four-link assumption precludes neighbouring mechanisms that may originate in monolithic arches. On the other hand, Uzman et al. [13] was among the first to apply optimisation methods to develop a recursive relationship for the design of parabolic and circular arches of varying cross section.

This work presents a MATLAB-based package that determines the minimum thickness and corresponding collapse mechanisms for arches of any form either monolithic or with voussoirs when subjected to concurrent gravity and seismic inertial loading. The programme allows the exploration of the different aspects influencing the minimum thickness of an arch subjected to inertial loading like the arch's aspect ratio, the magnitude of the inertial load as well as different gravitational fields. The software also allows the estimation of the imminent hinge locations associated with the likely collapse mechanism. Importantly, the effects of the gravitational acceleration are parametrised in terms of a gravitational multiplier (α) taken as a proportion of the terrestrial gravitational acceleration $g = 9.81$ m/s^2. In this way, (i) vertical seismic components; (ii) additional vertical loads and/or (iii) off-Earth gravitational fields can be considered.

2. Software description

### 2.1. Algorithm description

The numerical procedure for thrust-line analysis presented herein relies on the discretisation of the arch into a finite number of distinct *blocks* whose properties are summarised in Table 1. Each *block* is defined by the radial coordinates of its vertices, (r_i, θ_i). The algorithm contains the class definition for the object and takes as input the corners' polar coordinates and automatically generates the other properties based upon the density, gravitational acceleration, gravitational multiplier and lateral acceleration. Since an equivalent static approach to limit state analysis is adopted the static horizontal inertial load, F_h, is taken as the product of its area, density and lateral acceleration and assumed to act on the centroid of each block

A masonry arch can be simulated by means of a few blocks where each one of them represents an individual voussoir whereas a greater number of blocks can approximate a monolithic construction. Moreover, the arch's local thickness can be easily varied by changing the radial coordinates of the corresponding block. Besides, the Couplet–Heyman assumptions [1] are adopted including those of negligible tensile strength and that the structure must maintain stability through compression only paths [2,14].

Our algorithm also requires an initial estimation of the reaction forces at the arch springings. Previous work has relied on arbitrary distributions of vertical and horizontal forces e.g. [15]; instead, we employ the virtual work principle – by suppressing momentarily the Couplet–Heyman undeformability assumption [1] – in order to obtain initial estimates that are closer to physical realisability. These initial reaction estimates will be subsequently updated during the calculation process as described later in this paper.
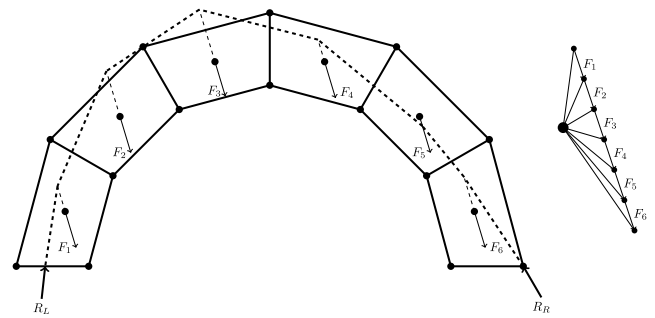
(a) Six-voussoir arch showing the funicular polygon (left) and its corresponding Force Polygon (right). Thick dashed line represents the Funicular Polygon under a ground acceleration of $0.3g$, whilst the thin dashed line represents the line of action of the resultant force (F_i) acting at each block's centroid.
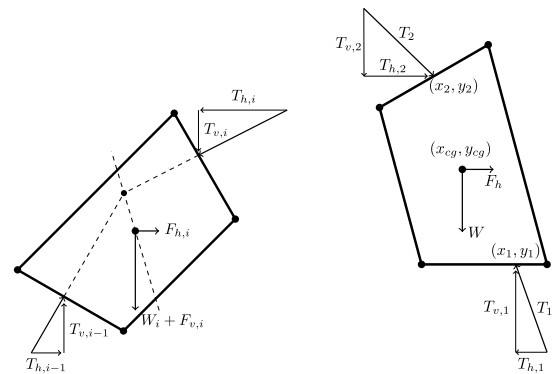
(b) Equilibrium of forces acting on Block i where $T_{h,i}$, $T_{v,i}$, $F_{h,i}$, $F_{v,i}$ and W_i are the horizontal thrust, vertical thrust, horizontal force, vertical force and self-weight of block i, respectively.

(c) Moment equilibrium of a block.

Fig. 1. Construction of the funicular polygon.

2.1.1. Construction of the funicular polygon

The funicular polygon defines the lines of action of the resultant thrust forces throughout the arch. This can be visualised by moving from left to right in Fig. 1(a) which depicts a six-voussoir arch subjected to its self-weight and constant horizontal (inertial) forces from left to right equivalent to a support acceleration of $0.3g$, where g is the terrestrial gravitational acceleration. The initial line of action is that of the reaction force, R_L, and the vertical components of the forces are incrementally reduced by the weight of each block until the final one is coincidental with the reaction force at the other side, R_R. This process is schematically shown in Fig. 1(b) for the ith block. A simple approach to constructing a funicular polygon is through the use of a force polygon that represents the equilibrium of forces within the structure [6,14].

2.1.2. Thrust-line construction

The many intricacies involved in obtaining an admissible thrust-line for non-classical forms can complicate the numerical calculation of the funicular polygon, especially when low-gravity conditions or extreme lateral forces are examined. Instead, a simpler and more robust approach based on the moment equilibrium of a block, as shown in Fig. 1(c), is followed herein. To

Table 1
Block properties.

| Computer variable	Definition
r	Radial coordinates (r_1, r_2, r_3, r_4)
theta	Angular coordinates $(\theta_1, \theta_2, \theta_3, \theta_4)$
density	Material density [kg/m³]
A	Area of the block [m²]
M	Mass of the block per unit width [kg/m]
W	Weight of the block per unit width [N/m]
r_cg	Radial coordinate of the centre of gravity (r_{cg})
theta_cg	Angular coordinate of the centre of gravity (θ_{cg})
Fh	inertial load per unit width due to ground acceleration [N/m]
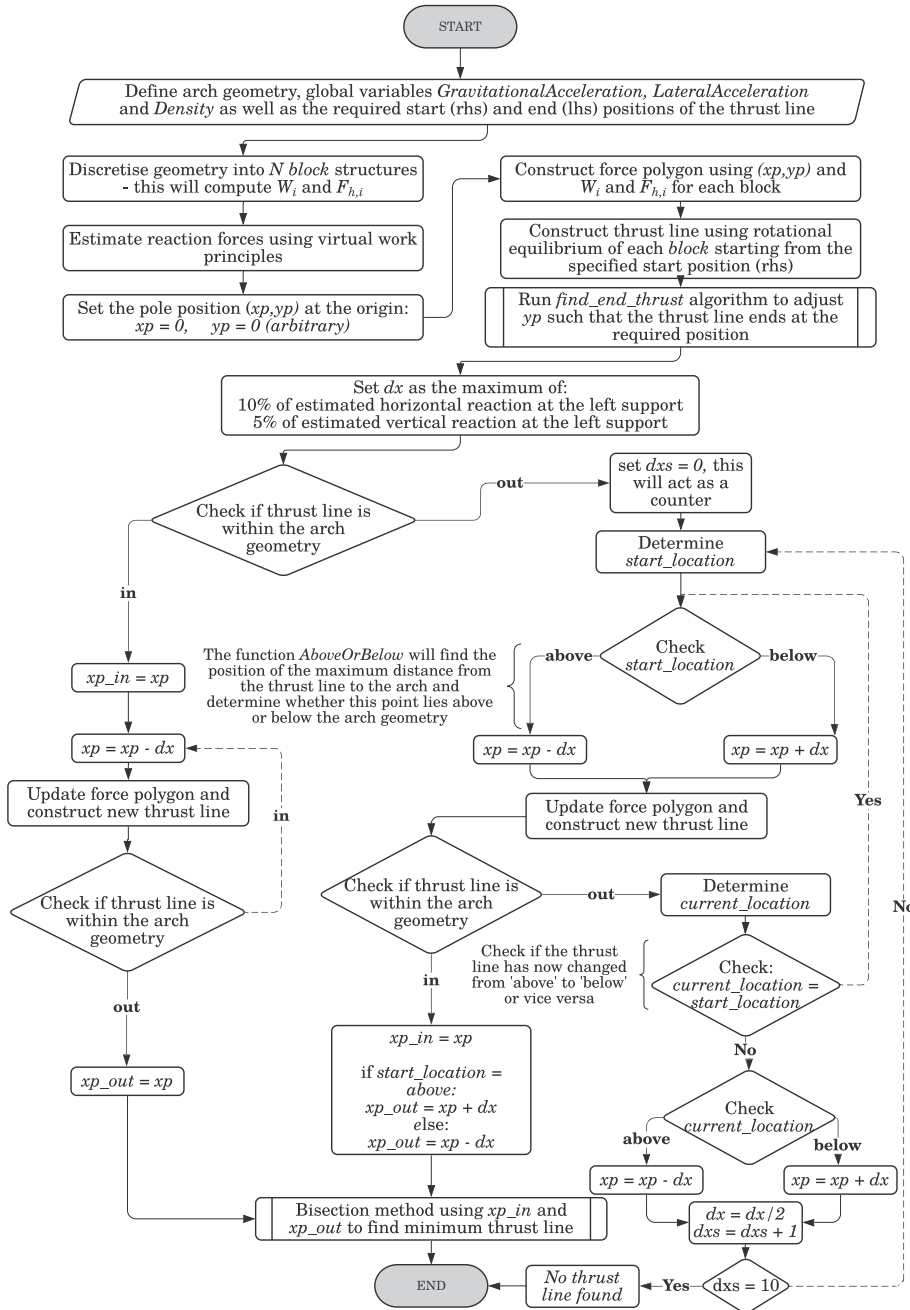
Fig. 2. Limit thrust-line algorithm.

this end, we recognise that the thrust components, T_1 and T_2, are known to satisfy horizontal and vertical equilibrium through the construction of the force polygon. Therefore, by assuming an initial point (x_1, y_1) the only unknown is coordinate pair (x_2, y_2).

First we take moment equilibrium about (x_{cg}, y_{cg}) with positive moments anticlockwise;

$$T_{v,2}x_{cg} + T_{h,2}y_{cg} + T_{v,1}(x_1 - x_{cg}) - T_{h,1}(y_{cg} - y_1) = T_{v,2}x_2 + T_{h,2}y_2 \quad (1)$$

Imposing that (x_2, y_2) must lie on the line defined by the top edge $y = mx + c$:

$$-c = mx_2 - y_2 \tag{2}$$

leads to:

$$\begin{bmatrix} a \\ -c \end{bmatrix} = \begin{bmatrix} T_{v,2} & T_{h,2} \\ m & -1 \end{bmatrix} \begin{Bmatrix} x_2 \\ y_2 \end{Bmatrix} \tag{3}$$

$$A = TX \implies X = T^{-1}A$$

where $a = T_{v,2}x_{cg} + T_{h,2}y_{cg} + T_{v,1}(x_1 - x_{cg}) - T_{h,1}(y_{cg} - y_1)$.

2.2. Limit thrust-line algorithm

The initial estimates of reaction forces, assumed to act at the mid point of each support and calculated through the virtual work principle, are a good first approximation but can lead to a non-admissible set of thrust forces (i.e giving a thrust-line that does not lie within the arch geometry). In order to converge to a feasible limit thrust-line an iterative procedure is required. To this end, our algorithm allows the user to specify a range of starting (right hand side) and end (left hand side) points of the thrust-line. These limits can be set on the basis of the thickness of the arch at its springings, the conditions of the abutments, or other project-specific design criteria. The vertical position of the force polygon pole, which controls the amount of vertical thrust in the system, will determine where the thrust line ends. Hence by iteratively adjusting the vertical position of the pole, a thrust-line (either admissible or non-admissible) can be found that starts and ends at the user's specified points. Similarly, the horizontal position of the force polygon pole controls the amount of horizontal thrust in the system, with more horizontal thrust creating 'flatter' thrust-lines. Using these principles, the horizontal position of the pole is iteratively adjusted to make it steeper or shallower until an admissible thrust-line is found. Once an admissible thrust-line is found, the bisection method is implemented to find the limiting thrust-line that lies just within the arch geometry. The detailed process is presented in Fig. 2.

2.3. Minimum thickness algorithm

The numerical framework set out above can be easily adapted into a minimum-thickness search procedure. To this end, we observe that the start and end points of an arch's minimum thrust-line under self-weight, are shifted to the right when horizontal inertial loads are applied from left to right As the horizontal loading is increased, the end points of the thrust lines will attain a limit position at the intrados on the left and at the extrados on the right (for a left-to-right lateral load). Evidence of this can be found in the collapse mechanisms presented in the literature, e.g. [6,16], including cases with embrace angles different than 180°. Assuming that this effect will occur in any arch of standard geometry provides a methodical way to search for a limiting thrust-line. Once the thrust-line has reached the intrados at the left support or the extrados at the right support, the hinges implied by these points will remain there. Thus, once this occurs, the start and end points can be assumed to be fixed; hence minimising the number of required iterations. However, this supposition may not hold for small lateral loads and more complex non-classical arch forms where this condition can be lifted, and additional iterations performed.

The first step to find the minimum thickness of arches subject to horizontal inertial loads is to analyse their stability under their own weight. To this end, the end and start points of the thrust-line should be set to ensure its symmetry. The thickness of the arch can then be iteratively reduced with a constant step size until no new admissible thrust-line can be found. Iteratively
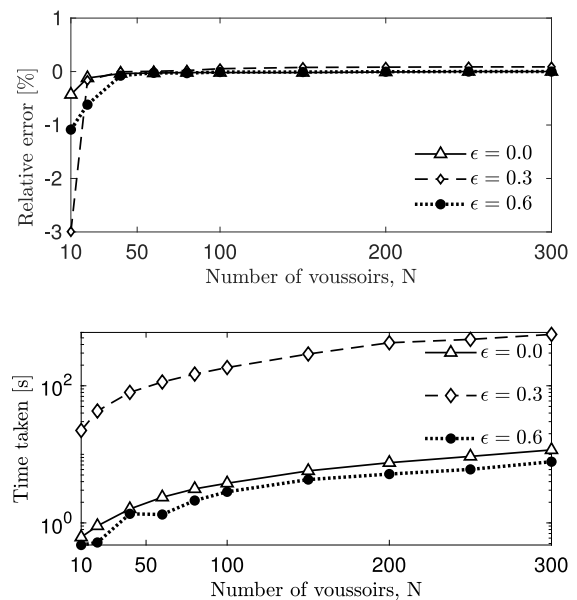

Fig. 3. Convergence of the minimum thickness calculation to analytical solutions [6] for semicircular arches. ϵ is the dimensionless inertia loading $\epsilon = \ddot{u}_g/g$ where $\ddot{u}_g$ is the ground acceleration.

repeating this with smaller step sizes will allow the minimum thickness to be found to a desired level of accuracy. The same process can be used to calculate the minimum thickness of an arch subject to horizontal inertial loading. However, in this case, for each starting point of the thrust-line at the right support, an additional step is implemented to allow the end point to move through the thickness of the left support. In this paper, minimum thicknesses, in terms of thickness over rise, t/R, are calculated to five decimal places to facilitate their comparison with analytical formulations, when available.

Fig. 3 shows the convergence of the minimum thickness algorithm described above. The relative error is calculated against the analytical results for semicircular arches given by Alexakis and Makris [6]. Three sets of results are presented for increasing levels of dimensionless inertial loading, $\epsilon = \ddot{u}_g/g$, where $\ddot{u}_g$ is the ground acceleration and $g = 9.81$ m/s² is the acceleration due to gravity on Earth. In the case of self-weight only, $\epsilon = 0$, and for $\epsilon = 0.6$ the start and end positions of the thrust-line were known a priori either at the extrados or intrados, and hence no iterations through the thickness of either support were required. In these two cases, the error quickly approximates 0% with only 40 blocks. In the case of $\epsilon = 0.3$ the position of the thrust-line at the left support is not known and therefore the algorithm has to search through its thickness. To this end, the left support was discretised into two hundred increments. These additional iterations cause an appreciable increase in the computational time and the algorithm converges to 0.09% relative error.

3. Validation against analytical results on classical arch forms

The thrust-lines and their corresponding minimum thicknesses outputs generated with OpenArch are compared against the analytical results provided by Alexakis and Makris [6] for semicircular arches and by Kampas et al. [16] for parabolic arches. Comparisons are established in terms of both minimum thickness and predicted hinge location for varying dimensionless inertial loading, $\epsilon = \ddot{u}_g/g$.
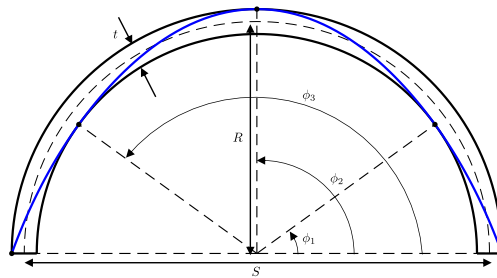
(a) Limit thrust-line of a semicircular arch under self-weight and hinge position conventions for semicircular arches.
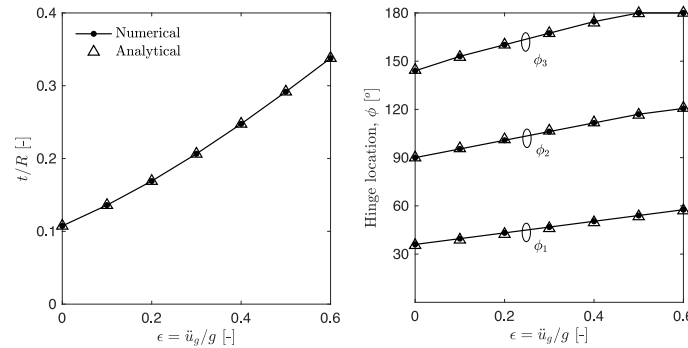
(b) Validation of minimum thickness to rise ratio (t/R) and hinge locations of semicircular arches subject to equivalent static inertial loading for a constant horizontal acceleration $\epsilon = \ddot{u}_g/g$ [-]. Curves corresponding to the same ϕ_i are tagged together with an ellipse.

Fig. 4. Semicircular arches of minimum thickness. Validation against analytical solution by Alexakis and Makris [6].

Table 2
Validation of the minimum thickness of semicircular arches subject to equivalent static loading for a constant horizontal acceleration $\epsilon = \ddot{u}_g/g$ [-] [6].

$\epsilon = \ddot{u}_g/g$	t/R (Analytical)	t/R (Numerical)	Relative error (%)
0.0	0.10748	0.10746	−0.02
0.1	0.13590	0.13597	0.05
0.2	0.16897	0.16908	0.07
0.3	0.20636	0.20648	0.06
0.4	0.24752	0.24758	0.02
0.5	0.29175	0.29170	−0.02
0.6	0.33788	0.33785	−0.01

Table 3
Validation of the minimum thickness of parabolic arches subject to equivalent static inertial loading for a constant horizontal acceleration $\epsilon = \ddot{u}_g/g$ [-] [16].

| $\epsilon = \ddot{u}_g/g$	t/R (Analytical)	t/R (Numerical)	Relative error (%)
0.00	0.023863	0.02386	−0.01
0.05	0.037963	0.03802	0.15
0.10	0.056831	0.05710	0.47
0.20	0.100109	0.10131	1.20
0.30	0.145416	0.14764	1.53
0.40	0.191623	0.19470	1.61
0.50	0.238416	0.24205	1.52
0.60	0.285692	0.28956	1.35
0.7916	0.377515	0.38097	0.92
1.0554	0.506764	0.50827	0.30
1.2048	0.581500	0.58195	0.08
1.3193	0.639596	0.63984	0.04

Semicircular arches

One hundred blocks with radial edges were used to accurately represent the geometry for a direct comparison with the analytical results of [6]. This relatively high discretisation was necessary

in order to achieve a reasonable estimate of the hinge locations as they can only occur at the discrete *block* edges. Fig. 4(a) presents the nomenclature and convention followed. Also, the start and end positions of the thrust-line were discretised into two hundred increments along the arch support thickness. Table 2 shows a comparison between the numerical and analytical results for minimum thickness ratios, t/R, while the hinge locations are shown in Fig. 4(b).

The numerical results presented in Table 2 and Fig. 4(b) show a very close match between our predictions and the analytical results. A maximum relative error in minimum thickness of 0.07% is observed for $\epsilon = 0.2$. These excellent results are also evident in the hinge locations, confirming that the estimated thrust-line has the correct shape. This is crucial as the shape of the thrust-line will form the basis of the form finding algorithm presented later in this paper.
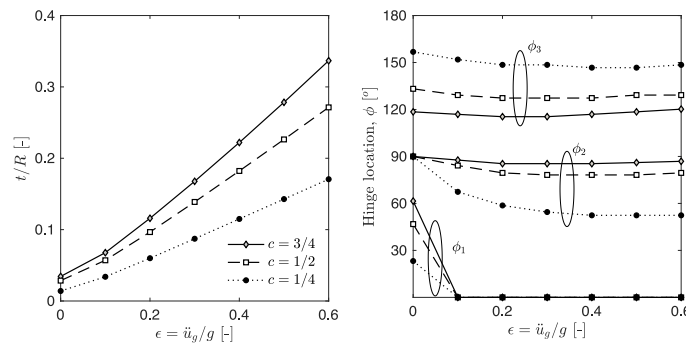
Parabolic arches

The analytical solutions provided by Kampas et al. [16] on parabolic arches were also used for validation purposes. Fig. 5(a) shows the convention adopted. Radial ruptures were assumed and five hundred blocks were employed in order to achieve a high level of accuracy given the relative complexity of the parabolic arch, with the crown of the arch being particularly steep. The study by Kampas et al. [16] is the first to consider the effect of low-gravity conditions on the minimum thickness and collapse mechanisms of parabolic arches. Simply put, low-gravity effectively amplifies the value of ϵ for a given level of "horizontal" inertial forces due to the reduced self-weight. To ensure that the algorithm is robust enough to cope with the effects of low gravity,
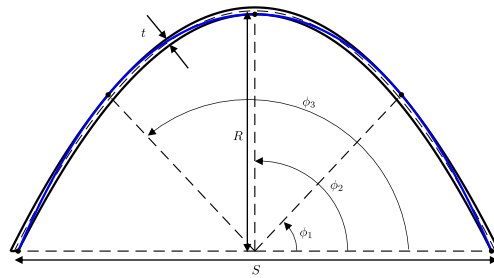
(a) Limit thrust-line of a parabolic arch under self-weight with aspect ratio $c = R/S$ and hinge position conventions for parabolic arches.
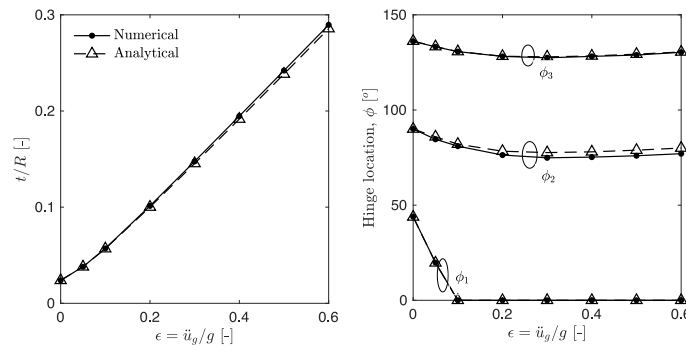
(b) Validation of minimum thickness to rise ratio (t/R) and hinge locations of parabolic arches subject to equivalent static inertial loading for a constant horizontal acceleration $\epsilon = \ddot{u}_g/g$ [-], where u_g is the ground acceleration. Validation against analytical solution by Kampas et al. [16]. Curves corresponding to the same ϕ_i are tagged together with an ellipse.

(c) Minimum thickness to rise ratio (t/R) and imminent hinge locations for parabolic arches of constant thickness subject to equivalent static inertial loading for a constant horizontal acceleration $\epsilon = \ddot{u}_g/g$ [-], where u_g is the ground acceleration. Curves corresponding to the same ϕ_i are tagged together with an ellipse.

Fig. 5. Parabolic arches of minimum thickness.

results for extreme loads have also been validated against the analytical results.

Table 3 and Fig. 5 show the minimum thickness and hinge locations calculated using the numerical approach alongside the analytical results. The relative error in minimum thickness increases from 0.01% in the self-weight case, to 1.61% at $\epsilon = 0.4$, before reducing to 0.04% at $\epsilon = 1.31926$. This is due to the

aforementioned steepness of the arch in the region of the crown. The numerical procedure predicts slightly lower hinge locations in the approach to this region, ϕ_2. This is because in this 'sensitive' region, a small change in angular coordinate has a relatively large effect on the radial coordinate. As the numerical approach under predicts the angle ϕ_2, its separation with ϕ_3 is greater. This
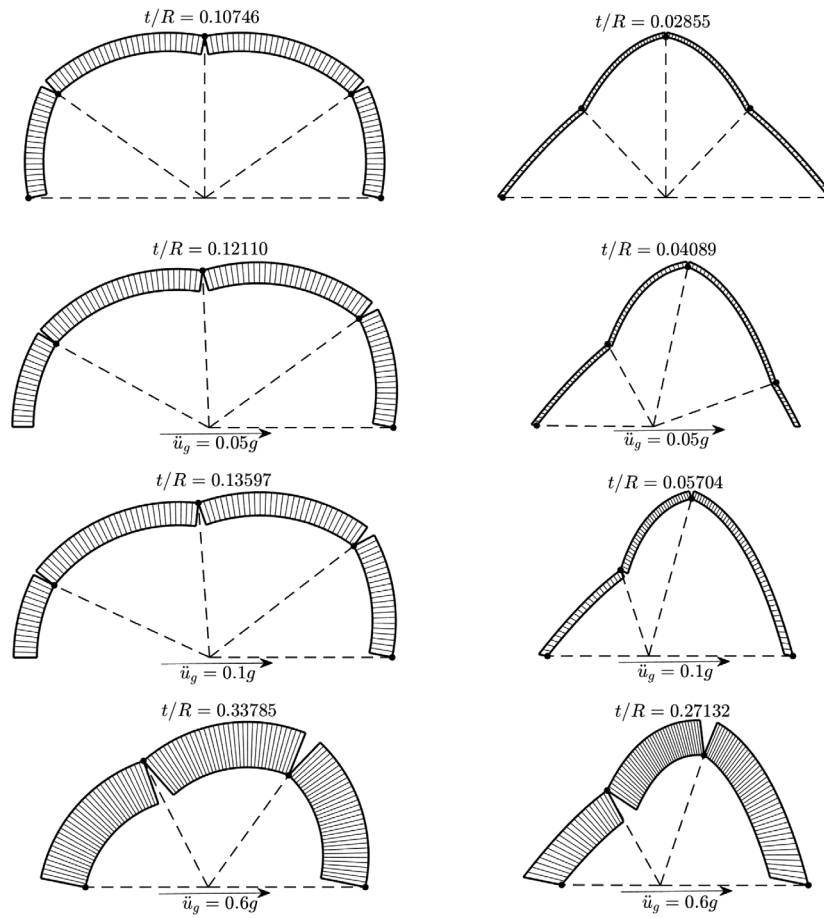
Fig. 6. Comparison of minimum-thickness semicircular and parabolic arch collapse mechanisms under self-weight and varying levels of constant horizontal acceleration $\epsilon = \ddot{u}_g/g$, where u_g is the ground acceleration and t/R the thickness to rise ratio.

greater separation between the two hinges is the cause for the slight overestimation of the minimum thickness.

Parabolic arches of constant thickness

The minimum thickness algorithm presented in Section 2.3 can be used to find solutions for arches of any geometry under different inertial loading. For example, there are multiple ways to define a parabolic arch as a radial cut through its midline is not necessarily perpendicular to it [16]. Or in other words, it is impossible to ensure both a constant thickness perpendicular to the midline and intrados and extrados that are of the same form. In particular, at least three options exist: (i) the intrados and extrados are defined by parabolas analogous to the centre line, (ii) a constant thickness perpendicular to the midline is assumed, and (iii) a constant radial thickness is assumed (for the given point of reference). Whilst the difference in geometry between these three options is small, they will lead to different estimates of minimum thickness and hinge locations. Besides, Makris and Alexakis [4] have demonstrated that the thrust-line adopts different shapes depending on the stereotomy of the arch.

In this section, parabolic arches of constant thickness perpendicular to their midline are examined. These arches behave in a manner almost identical to the parabolic arches with radial cuts validated in the previous section, albeit with a small reduction in minimum thickness. These results, calculated using one hundred blocks with radial edges, are presented in Fig. 5(c). The same naming conventions presented before in Fig. 5(a) hold.

The immediately striking result, is that parabolic arches are far more efficient than semicircular arches under lower loading.

When subjected to their self-weight only, the thickness of a semicircular arch is approximately 11% of its rise compared to 2.4% for a parabolic arch (see Tables 2 and 3). The dramatically thinner parabolic arches under smaller loads also result in different collapse mechanisms to those of a semicircular arch under the same conditions. This feature is explored further in Fig. 6 which shows a comparison of the collapse mechanisms of semicircular and parabolic arches of minimum thickness under various loading conditions. In complete contrast to the semicircular case, ϕ_1 and ϕ_3 correspond to extrados hinges whilst ϕ_2 and the springing hinges occur at the intrados. This difference causes the parabolic arch to buckle inwards under its own weight compared to outwards in the case of the semicircular arch. Despite this initial difference, under a high enough lateral loading, both geometries converge to the same two-springing four hinge mechanism identified by Alexakis and Makris [6]. In the transition to this state, ϕ_1 of the parabolic arch rotates clockwise to the extrados of the right springing. This is evidenced by the hinge rotations presented in Fig. 5(c) where shortly after ϕ_1 hits the springing, ϕ_2 and ϕ_3 begin to reverse direction.

4. Impact

The stability of arches subjected to concurrent seismic and vertical loads is a foundational problem in structural mechanics. Arches are versatile and elegant structures that are ubiquitous in civil infrastructure from vernacular constructions to the most recently proposed extraterrestrial habitats [17]. The software package presented here enables a quick and precise estimation of

the minimum-thickness associated with a stable behaviour of these structures and their corresponding failure mechanism. The specification of the problem parameters is straightforward and the code is user-friendly. The code has been validated against available analytical solutions and it has already been used to gain insight into the mechanics of arches of the parabolic shape in [16]. Moreover, the software can be incorporated into form-finding algorithms for the easy exploration of more advanced geometries like in [18]. All these features make OpenArch a useful tool for researchers and engineers interested in the design of optimal structures.

5. Conclusions

This paper has described the implementation and features of the OpenArch software package for the identification of minimum-thickness arches of any geometry and their corresponding collapse mechanisms under seismic action. The outputs of the software have been validated against analytical formulations available in the scientific literature. This has shown the capabilities of the code in addressing classical geometries, although the code can operate with arches of more complex configurations. In this regard, no constant thickness requirements are hard-coded into OpenArch, and it is expected that it can be used in the exploration of non-standard arch forms under extreme loading by engineers and researchers alike.

Declaration of competing interest

The authors declare that they have no known competing financial interests or personal relationships that could have appeared to influence the work reported in this paper.

Acknowledgements

References

[1] Heyman J. The stone skeleton. Int J Solids Struct 1966;2(2):249–79. http://dx.doi.org/10.1016/0020-7683(66)90018-7.

[2] Benvenuto E. An introduction to the history of structural mechanics. volume II: vaulted structures and elastic systems. Berlin, New York: Springer-Verlag; 1991.

[3] Milankovitch M. Beitrag zur theorie der druckkurven (PhD thesis), Vienna: Dissertation zur Erlangung der Doktorwürde, KK technische Hochschule; 1904.

[4] Makris N, Alexakis H. The effect of stereotomy on the shape of the thrust-line and the minimum thickness of semicircular masonry arches. Arch Appl Mech 2013;83(10):1511–33. http://dx.doi.org/10.1007/s00419-013-0763-4.

[5] Nikolić D. Catenary arch of finite thickness as the optimal arch shape. Struct Multidiscip Optim 2019;60(5):1957–66. http://dx.doi.org/10.1007/s00158-019-02304-9.

[6] Alexakis H, Makris N. Limit equilibrium analysis and the minimum thickness of circular masonry arches to withstand lateral inertial loading. Arch Appl Mech 2014;84(5):757–72. http://dx.doi.org/10.1007/s00419-014-0831-4.

[7] Gáspár O, Sipos AA, Sajtos I. Effect of stereotomy on the lower bound value of minimum thickness of semi-circular masonry arches. Int J Archit Heritage 2018;12(6):899–921. http://dx.doi.org/10.1080/15583058.2017.1422572.

[8] Sacco E. Some aspects on the statics of masonry arches. In: Masonry structures: between mechanics and architecture. Springer; 2015, p. 265–90. http://dx.doi.org/10.1007/978-3-319-13003-3_10.

[9] Ricci E, Fraddosio A, Piccioni MD, Sacco E. A new numerical approach for determining optimal thrust curves of masonry arches. Eur J Mech A Solids 2019;75:426–42. http://dx.doi.org/10.1016/j.euromechsol.2019.02.003.

[10] Stockdale G, Tiberti S, Camilletti D, Papa GS, Habieb AB, Bertolesi E, Milani G, Casolo S. Kinematic collapse load calculator: Circular arches. SoftwareX 2018;7:174–9. http://dx.doi.org/10.1016/j.softx.2018.05.006.

[11] Zampieri P, Amoroso M, Pellegrino C. The masonry buttressed arch on spreading support. In: Structures, vol. 20. Elsevier; 2019, p. 226–36. http://dx.doi.org/10.1016/j.istruc.2019.03.008.

[12] Oppenheim IJ. The masonry arch as a four-link mechanism under base motion. Earthq Eng Struct Dyn 1992;21(11):1005–17. http://dx.doi.org/10.1002/eqe.4290211105.

[13] Uzman U, Daloglu A, Saka MP. Optimum design of parabolic and circular arches with varying cross section. Struct Eng Mech: Int J 1999;8(5):465–76. http://dx.doi.org/10.12989/sem.1999.8.5.465.

[14] Block P, DeJong M, Ochsendorf J. As hangs the flexible line: Equilibrium of masonry arches. Nexus Netw J 2006;8(2):13–24. http://dx.doi.org/10.1007/s00004-006-0015-9.

[15] Michiels T, Adriaenssens S. Form-finding algorithm for masonry arches subjected to in-plane earthquake loading. Comput Struct 2018;195:85–98. http://dx.doi.org/10.1016/j.compstruc.2017.10.001.

[16] Kampas G, Kalapodis N, McLean T, Málaga-Chuquitaype C. Limit-state analysis of parabolic arches subjected to inertial loading in different gravitational fields using a variational formulation. Eng Struct 2021;228:111501. http://dx.doi.org/10.1016/j.engstruct.2020.111501.

[17] Kalapodis N, Kampas G, Ktenidou O-J. A review towards the design of extraterrestrial structures: From regolith to human outposts. Acta Astronaut 2020;175:540–69. http://dx.doi.org/10.1016/j.actaastro.2020.05.038.

[18] McLean T. Optimal forms of regolith-based arches subject to inertial loading in low-gravity conditions. MEng dissertation, Imperial College London; 2020.